Journal of Photochemistry, 6 (1976/77) 439 - 452

RKR FRANCK–CONDON FACTORS AND ABSORPTION CROSS-SECTIONS FOR ROTATIONAL TRANSITIONS IN THE $A^2\Pi_i$–$X^2\Pi_i$ SYSTEM OF ClO

J. A. COXON

Department of Chemistry, Dalhousie University, Halifax, Nova Scotia B3H 4J3 (Canada)

(Received November 11, 1976)

Summary

Available spectroscopic data are used to obtain RKR potential energy curves for the $A^2\Pi_i$ and $X^2\Pi_i$ states of ClO. Franck–Condon factors for the A–X system are reported. With the recent revision in the A state vibrational numbering, the results are more reliable than those of previous work with Morse potentials. The known line-widths and calculated line strengths for the A–X bands are used in computer generation of absorption cross-section profiles for individual bands. The cross-sections are obtained on an absolute basis by computer simulation of band head extinction coefficient measurements. A simple procedure is described for the calculation of photolysis rates in the banded region of ClO (A ← X).

Introduction

The $A^2\Pi_i \leftarrow X^2\Pi_i$ ultra-violet absorption system of ClO is characterized by a progression of $^2\Pi_{3/2} \leftarrow {}^2\Pi_{3/2}$ sub-bands from $v'' = 0$, which leads to a continuum beyond the convergence limit at 263 nm. Following the first identification [1] of ClO from observation of the A–X system in emission, there has been considerable interest in the kinetics of reactions which produce and remove the radical. In many studies [2 - 7], measurements of absorption intensities, either in the continuum or banded regions of the A–X system, have been used to follow ClO concentrations. In the case of band absorption, however, extinction coefficient determinations have been empirical, or, apparent quantities which depend on the spectral bandwidth employed and the temperature of the ClO absorber. For this reason, it has been difficult to make reliable comparisons of data from different studies, and it is clear that information on the Franck–Condon factors and detailed absorption cross-sections would be of much value in the interpretation of intensity data for ClO (A–X).

A recent interest in the spectroscopy and reaction kinetics of ClO has followed the suggestion of Molina and Rowland [8] that significant depletion

of stratospheric ozone might arise from the introduction of chlorofluorocarbons and other chlorine-containing compounds into the earth's atmosphere. Of the numerous elementary reactions which are considered in discussions of the detailed chemistry, formation and loss processes of ClO play a crucial role, even though the steady-state concentrations are expected to be much less than the total concentration of all active chlorine-containing species (mostly HCl) [9]. Since the reliability of the complex kinetic and transport models is best established by comparison of predicted concentrations with measured values, there is much interest in techniques for measurement of [ClO] in the stratosphere. One possibility is detection by ultraviolet absorption. It is unfortunate however that absorption by ozone precludes the possibility of measurements for the strongest bands near 280 nm, and limits such experiments to wavelengths longer than ~300 nm where the ClO (A–X) Franck–Condon factors are low.

In order to facilitate such investigations, Nicholls [10] has recently published an array of Franck–Condon factors which were based on Morse potentials for both states. However, in addition to the errors known to be associated with the use of Morse curves as approximations for the real potentials, especially for transitions remote from the principal Condon parabola, more serious criticisms can be noted which diminish the reliability of the results reported by Nicholls. First, it has been established [11] that the previously accepted vibrational numbering in the $A^2\Pi_i$ state is in error and should be decreased by one unit; and secondly, a recent reinvestigation [12] of the A–X absorption bands at high resolution has led to a different set of rotational constants for the A state than those found in the earlier work of Durie and Ramsay [13].

In the present work, the available spectroscopic data on ClO have been used to construct RKR curves for the X and A states. Franck–Condon factors for the A–X system were calculated from wavefunctions found by numerical solution of the radial wave equation. Finally using known linewidths and calculated line strengths, absolute absorption cross-sections are reported for the 11–0 band (which has the largest Franck–Condon factor) and for the much weaker 2–0, 3–0 and 4–0 bands, which are the optimum cases for stratospheric measurements. Account is taken of a recent *ab initio* calculation of the transition moment variation [14].

RKR potential energy curves

The calculation of RKR curves for the A and X states of ClO was less straightforward and less accurate than is usual in work of this type. The calculations were based on recent data obtained from analyses of high resolution spectra of the A–X absorption [12] and emission [15] bands. However, the A state is predissociated in every observed level (but to varying extents), and the large linewidths introduce considerable error in the rotational constants, principally from blending. In addition, most of the data were obtained

for the $^2\Pi_{3/2}$–$^2\Pi_{3/2}$ sub-system, so that the rotational constants are only effective values which contain contributions from the spin-orbit interaction. Although it is difficult to estimate the magnitude of errors caused by these effects, the RKR curves given below are the best that can be obtained from the available data, and they should be considerably more reliable than Morse curves.

For the ground state, the differences, $B''_{v2}-B''_{v1}$, between the effective rotational constants for the $^2\Pi_{1/2}$ and $^2\Pi_{3/2}$ components are not expected to show a large variation with v'' for the lowest vibrational levels. It was assumed, therefore, that the accurately known difference for $v'' = 0$ from the microwave spectrum of ClO [16] could also be used for $v'' \leqslant 9$, for which only the B''_{v1} values have been found. It was assumed further that the means of B''_{v2} are close to the mechanical B''_v values. The vibrational term values were obtained from the constants given by Coxon *et al.* [15].

A similar, but less satisfactory procedure was adopted for the A state. In this case, there are no microwave data, and the results from the electronic spectrum for $v' \leqslant 4$ suggest that $B'_{v2}-B'_{v1}$ decrease quite rapidly with v'. For $v' = 9$, the experimental value for B'_{v2} is actually less than for B'_{v1}, but this result may be associated with the perturbation in the $^2\Pi_{1/2}$, $v' = 9$ level [12]. For the present purpose, it was assumed that $B'_{v2}-B'_{v1}$ decreases steadily for $v' \leqslant 8$, while the mean of B'_{v2} and B'_{v1} was used for $v' = 9$. The vibrational terms were obtained again from the known constants [15]. The situation in the smaller energy range for $v' \geqslant 10$ is even less satisfactory since there are no data for the $^2\Pi_{1/2}$ component. However, the differences between B'_{v1} and B'_{v2} are not large for $v' \leqslant 9$, and it is probable that the B_{v1} values are close to the mechanical constants also for $v' \geqslant 10$. Similarly, it can be assumed that the vibrational intervals observed for the $^2\Pi_{3/2}$ sub-bands are close to the true intervals. On this basis, a second RKR curve was calculated which made use of only the data for $A^2\Pi_{3/2}$. Since the turning points for the two curves were in close agreement for $v' = 9$, it was considered a good approximation to adopt the $^2\Pi_{3/2}$ curve for the higher levels with $v' \geqslant 10$. The RKR turning points for the A and X states of ClO, calculated using the method described previously [17, 18], are given in Table 1. It should be noted, however, that the results for $v' \geqslant 16$ of the A state are smoothed values. The need for smoothing is illustrated in Fig. 1, which shows a plot of the r_{min} limb for the $A^2\Pi$ state. While the RKR points for $v' \leqslant 15$ lie on a smooth curve, some small systematic error is evident at the highest energies. Discontinuities of this type are not uncommon for the few cases where RKR curves have been calculated to a dissociation limit, and are considered to arise from small errors in the rotational constants. It is assumed that the r_{min} limb can be extrapolated over the short range of r, thus requiring corresponding small corrections to the RKR values for the r_{max} limb also.

Franck–Condon factors and *R*-centroids

The RKR potentials described in the previous section were used in the calculation of Franck–Condon factors and r-centroids for ClO (A–X). In

TABLE 1

Turning points for the $A^2\Pi_i$ and $X^2\Pi_i$ states of ClO.

	$A^2\Pi$			$X^2\Pi$		
v	$U(r)$ (cm^{-1})	r_{min} (Å)	r_{max} (Å)	$U(r)$ (cm^{-1})	r_{min} (Å)	r_{max} (Å)
0	257.6	1.786	1.941	425.68	1.5131	1.6334
1	762.3	1.740	2.011	1268.47	1.4758	1.6854
2	1251.5	1.711	2.066	2100.11	1.4521	1.7241
3	1724.6	1.690	2.115	2920.5	1.4338	1.7574
4	2180.9	1.672	2.162	3729.5	1.4187	1.7878
5	2619.7	1.658	2.208	4527.0	1.4058	1.8163
6	3040.4	1.645	2.254	5312.9	1.3945	1.8435
7	3442.3	1.634	2.301	6086.9	1.3844	1.8697
8	3824.8	1.625	2.349	6849.1	1.3752	1.8952
9	4187.2	1.617	2.399	7599.3	1.3669	1.9202
10	4526.8	1.607	2.454			
11	4842.9	1.601	2.508			
12	5134.1	1.596	2.573			
13	5399.2	1.591	2.641			
14	5638.4	1.585	2.716			
15	5853.1	1.582	2.799			
16	6041.2	1.578	2.898			
17	6204.5	1.575	3.004			
18	6342.4	1.573	3.135			
19	6458.5	1.571	3.276			
20	6554.2	1.569	3.447			
21	6630.8	1.568	3.651			
22	6691.3	1.567	3.884			
23	6737.5	1.566	4.181			
24	6771.5	1.566	4.545			
25	6795.2	1.565	5.026			

most applications, results are required principally for the $^2\Pi_{3/2}$–$^2\Pi_{3/2}$ sub-bands, and while the Franck–Condon factors for the two sub-systems are very similar, account has been taken of the significant variation [15] of the spin-orbit coupling operator $A''(r)$. The quantity $1/2\ A''(r)$ was thus added to the potential for the $X^2\Pi$ ground state in Table 1. The corresponding variation of $A'(r)$ for the excited state is much lower, and was neglected in view of the greater uncertainties mentioned above. The numerical integrations were performed for 4000 points in the range 1.1 to 7.4 Å using standard techniques [19, 20]. Part of the matrix of Franck–Condon factors and r-centroids for ClO ($A^2\Pi_{3/2}$–$X^2\Pi_{3/2}$) is given in Tables 2 and 3, and includes

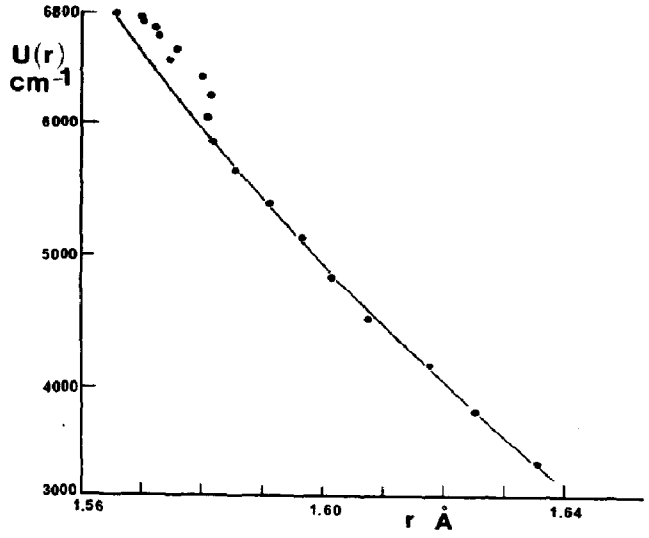

Fig. 1. The r_{min} limb for the $A^2\Pi$ state of ClO. •, RKR points.

all transitions likely to be observed in absorption or emission. The results are in good agreement with experimentally observed intensity distributions, and show that for absorption from $v'' = 0$, the banded region accounts for about half the total intensity of absorption.

Absorption cross-sections

Measurements of intensities of absorption are always made over a finite frequency range centred around a nominal frequency ν_0. Denoting the frequency dependence of the intensity of the source radiation as $J(\nu)$, the intensity of transmitted radiation (I_t) is related to the intensity of incident radiation (I_i) by the expression,

$$\frac{I_t(\nu_0)}{I_i(\nu_0)} = \frac{\int_{\nu_0 - \Delta\nu/2}^{\nu_0 + \Delta\nu/2} J(\nu) e^{-\sigma(\nu)N} \, d\nu}{\int_{\nu_0 - \Delta\nu/2}^{\nu_0 + \Delta\nu/2} J(\nu) \, d\nu} \tag{1}$$

In eqn. (1), N is the number of absorbers per unit cross-section and $\sigma(\nu)$ is the absorption cross-section. In the case of absorption due to overlapping lines in a single $v'-v''$ band, $\sigma(\nu)$ is the resultant of the cross-sections for the individual transitions between pairs of levels J' and J'',

$$\sigma(\nu) = \sum_{\substack{\text{all} \\ \text{lines}}} \sigma_{v'J'}^{v''J''}(\nu) \tag{2}$$

TABLE 2

Linewidths, Franck–Condon factors and r-centroids for the $v'' = 0, 1, 2$ progressions of ^{35}ClO ($A^2\Pi_{3/2}$–$X^2\Pi_{3/2}$).

		$v'' = 0$		$v'' = 1$		$v'' = 2$	
v'	$\delta\nu$ (cm^{-1})	q	$\bar{r}$ (Å)	q	$\bar{r}$ (Å)	q	$\bar{r}$ (Å)
0	1.4	0.0001	1.705	0.0013	1.725	0.0075	1.745
1	~7	0.0007	1.693	0.0067	1.712	0.0290	1.732
2	1.7	0.0023	1.682	0.0177	1.700	0.0575	1.719
3	2.5	0.0054	1.671	0.0331	1.689	0.0784	1.708
4	1.5	0.0101	1.661	0.0488	1.679	0.0810	1.696
5	2.9	0.0162	1.652	0.0605	1.669	0.0665	1.686
6	>5	0.0228	1.643	0.0655	1.660	0.0436	1.676
7	1.5	0.0292	1.635	0.0637	1.651	0.0220	1.665
8	2.1	0.0349	1.628	0.0566	1.643	0.0073	1.655
9	2.1	0.0391	1.620	0.0465	1.635	0.0007	1.634
10	3.1	0.0417	1.614	0.0354	1.628	0.0005	1.666
11	2.2	0.0428	1.608	0.0254	1.622	0.0039	1.646
12	1.9	0.0421	1.603	0.0169	1.616	0.0083	1.637
13	2.6	0.0393	1.598	0.0103	1.610	0.0117	1.631
14	1.4	0.0373	1.593	0.0061	1.605	0.0142	1.626
15	1.1	0.0330	1.589	0.0032	1.600	0.0147	1.621
16	1.0	0.0293	1.586	0.0015	1.594	0.0143	1.617
17	0.7	0.0248	1.583	0.0006	1.588	0.0128	1.614
18	0.9	0.0209	1.581	0.0002	1.580	0.0111	1.611
19	0.3	0.0173	1.579	—	—	0.0093	1.608
20	0.4_5	0.0141	1.577	—	—	0.0076	1.606
21	0.5	0.0109	1.576	—	—	0.0059	1.605
22	0.5	0.0086	1.575	—	—	0.0046	1.604
23	0.5	0.0063	1.574	—	—	0.0034	1.603

TABLE 3

Franck–Condon factors and r-centroids for the $v' = 0, 1, 2$ progressions of ^{35}ClO ($A^2\Pi_{3/2}$–$X^2\Pi_{3/2}$).

	$v' = 0$		$v' = 1$		$v' = 2$	
v''	q	$\bar{r}$ (Å)	q	$\bar{r}$ (Å)	q	$\bar{r}$ (Å)
0	0.0001	1.705	0.0007	1.693	0.0023	1.682
1	0.0013	1.725	0.0067	1.712	0.0177	1.700
2	0.0075	1.745	0.0290	1.732	0.0575	1.719
3	0.0264	1.766	0.0728	1.752	0.0977	1.739
4	0.0651	1.789	0.1154	1.773	0.0846	1.759
5	0.1194	1.812	0.1133	1.795	0.0238	1.777
6	0.1689	1.836	0.0577	1.817	0.0026	1.821
7	0.1889	1.861	0.0048	1.830	0.0532	1.831
8	0.1698	1.887	0.0163	1.878	0.0865	1.852
9	0.1246	1.915	0.0859	1.900	0.0437	1.874
10	0.075	1.942	0.140	1.924	0.001	1.869
11	0.037	1.972	0.147	1.952	0.030	1.938
12	0.015	2.003	0.109	1.982	0.102	1.964

In turn, $\sigma_{v''J''}^{v'J'}(\nu)$ are related according to:

$$\sigma_{v''J''}^{v'J'}(\nu) = \frac{L_{v''}^{v'}(\nu, \nu_{J''}^{J'})\, N_{J''}\, S_{J''}^{J'}}{N_{v''}\, g_{J''}} \tag{3}$$

where $L_{v''}^{v'}(\nu,\nu_{J''}^{J'})$ is a function which describes the lineshapes, $N_{J''}/N_{v''}$ is the fraction of molecules in the v'' level populating the J'' state, $S_{J''}^{J'}$ is the line strength, and $g_{J''}$ is the degeneracy. The fractional population $N_{J''}/N_{v''}$ is given by:

$$N_{J''}/N_{v''} = \frac{2J'' + 1}{Q_{\text{rot}}''}\, e^{-F(J'')/kT} \tag{4}$$

where $F(J'')$ is the rotational energy and Q_{rot}'' is the ground state rotational partition function. With $g_{J''} = 2J'' + 1$, substitution in eqn. (3) gives:

$$\sigma_{v''J''}^{v'J'}(\nu) = \frac{L_{v''}^{v'}(\nu,\nu_{J''}^{J'})\, S_{J''}^{J'}\, e^{-F(J'')/kT}}{Q_{\text{rot}}''} \tag{5}$$

In the present work, a Lorentzian line shape is used for the predissociately-broadened lines of the A–X system of ClO; in this case, $L_{v''}^{v'}(\nu,\nu_{J''}^{J'})$ is given by:

$$L_{v''}^{v'}(\nu, \nu_{J''}^{J'}) = \sigma_{v''}^{v'} \left[\frac{(\delta\nu/2)^2}{(\nu - \nu_{J''}^{J'})^2 + (\delta\nu/2)^2}\right] \tag{6}$$

where $\delta\nu$ is the linewidth at half maximum. It is noted, however, that in the case of broad, heavily overlapped lines, the cross-section profile is insensitive to the lineshape function; this was verified in calculations similar to those described below, but in which a triangular lineshape was used for the absorption close to the band heads.

Equations (2 - 6) have been used to generate absorption cross-section profiles for several $v'' = 0\,^2\Pi_{3/2} - {}^2\Pi_{3/2}$ sub-bands of ClO (A–X). These profiles permitted the calculation of absorption intensities (with intensities defined as photon fluxes) according to eqn. (1), but with $J(\nu)$ assumed constant for individual bands. In this case, the intensity of absorption is given by:

$$\frac{I_t(\nu_0)}{I_i(\nu_0)} = \frac{\int_{\nu_0 - \Delta\nu/2}^{\nu_0 + \Delta\nu/2} e^{-\sigma(\nu)N}\, d\nu}{\Delta\nu}$$

This approximation gave closely similar results to those for a triangular $J(\nu)$ slit function of halfwidth $\Delta\nu$. Relative rotational populations of the $v'' = 0$ level of the $^2\Pi_{3/2}$ component, as given by $(2J'' + 1)\, e^{-B_{01}''(J'' + 1/2)^2/kT}$ were calculated for 200 and 300 K. The value of B_{01}'' is 0.619773 cm^{-1} [12]. Rotational line strengths were obtained from the equations given by Kovács [21]. As expected, the line strengths were insensitive to the value of $Y_v' = A_v'/B_v'$ since the coupling is close to Hund's case (a) over all vibrational levels. The results are given in Table 4, together with the corresponding values at 300 K of $X_{J''}^{J'} = S_{J''}^{J'}\, e^{-F(J'')/kT}$, the relative cross-sections (eqn. 5). The corresponding partition functions are Q_{rot}'' (200 K) = 226.12 and Q_{rot}'' (300 K) = 338.25. Table 4 shows that the Q-branch contributions are small, especially for high J, in agreement with the experimental spectrum [12].

TABLE 4

Line strengths (S), and relative rotational populations (N) and cross-sections (X) for ClO $A^2\Pi_{3/2}$–$X^2\Pi_{3/2}$

J''	$S^P(J'')$	$S^Q(J'')$	$S^R(J'')$	$N_{J''}^{200}$	$N_{J''}^{300}$	$X_{300}^P(J'')$	$X_{300}^R(J'')$
1.5			1.60	4.00	4.00		1.60
2.5	1.60	1.54	2.86	5.87	5.91	1.57	2.82
3.5	2.86	1.14	4.00	7.58	7.72	2.76	3.86
4.5	4.00	0.91	5.09	9.11	9.39	3.76	4.78
5.5	5.09	0.76	6.15	10.40	10.91	4.63	5.59
6.5	6.15	0.65	7.20	11.45	12.25	5.38	6.30
7.5	7.20	0.56	8.23	12.24	13.39	6.02	6.89
8.5	8.23	0.50	9.26	12.77	14.32	6.55	7.37
9.5	9.26	0.45	10.28	13.03	15.03	6.96	7.73
10.5	10.28	0.41	11.30	13.06	15.54	7.26	7.98
11.5	11.30	0.38	12.32	12.85	15.83	7.45	8.13
12.5	12.32	0.35	13.33	12.46	15.92	7.54	8.16
13.5	13.33	0.32	14.34	11.89	15.82	7.53	8.10
14.5	14.34	0.30	15.35	11.20	15.55	7.43	7.96
15.5	15.35	0.28	16.36	10.40	15.13	7.26	7.73
16.5	16.36	0.26	17.36	9.54	14.57	7.01	7.44
17.5	17.36	0.25	18.37	8.64	13.90	6.70	7.09
18.5	18.37	0.24	19.37	7.73	13.14	6.36	6.70
19.5	19.37	0.22	20.38	6.84	12.32	5.97	6.28
20.5	20.38	0.21	21.38	5.98	11.45	5.56	5.83
21.5	21.38	0.20	22.38	5.17	10.56	5.13	5.37
22.5	22.38	0.20	23.39	4.42	9.96	4.70	4.91
23.5	23.38	0.19	24.39	3.74	8.76	4.27	4.45
24.5	24.38	0.18	25.39	3.13	7.89	3.85	4.01
25.5	25.38	0.17	26.39	2.60	7.05	3.44	3.58
26.5	26.38	0.17	27.39	2.13	6.25	3.05	3.17
27.5	27.38	0.16	28.39	1.73	5.51	2.69	2.79
28.5	28.38	0.15	29.39	1.39	4.82	2.36	2.44
29.5	29.38	0.15	30.39	1.10	4.18	2.05	2.12
30.5	30.38	0.14	31.38	0.87	3.60	1.77	1.82
31.5	31.38	0.14	32.38	0.68	3.08	1.51	1.56
32.5	32.37	0.14	33.38	0.52	2.62	1.29	1.33
33.5	33.37	0.13	1.38	0.40	2.21	1.09	1.12
34.5	34.37	0.13	35.37	0.30	1.86	0.91	0.94

The ClO(A–X) linewidths reported by Coxon and Ramsay [12], and listed here in Table 2, were visual estimates of the spreading of the lines on photographic enlargements. As a first step in the present work, it was decided to investigate how such visual estimates are related to the true linewidths at half maximum ($\delta\nu$). This was accomplished by computer syntheses of the cross-section profile for the 11–0 $^2\Pi_{3/2}$–$^2\Pi_{3/2}$ sub-band at 300 K. Runs were performed for $\delta\nu$ = 1.5, 2.0 and 2.5 cm^{-1}, and it was found that the appearance of the absorption spectrum at high resolution is sensitive to the linewidth. For example, the P-branch would only be resolved for $J'' > 6.5$, 8.5 and 10.5 for $\delta\nu$ = 1.5, 2.0 and 2.5 cm^{-1} respectively. Similarly, resolution in

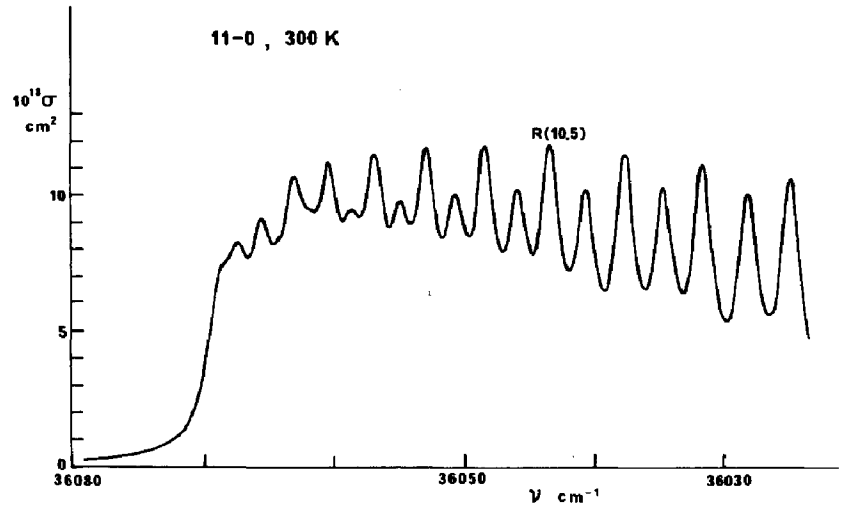

Fig. 2. Computed absorption cross-sections for the 11–0 ^{35}ClO ($A^2\Pi_{3/2}$–$X^2\Pi_{3/2}$) sub-band at 300 K. Linewidth = 2.0 cm^{-1}.

the R-branch could be expected for $J'' > 4.5$, 5.5 and 7.5. The profile for $\delta\nu$ = 2.0 cm^{-1} shown in Fig. 2 gives a particularly good match with the experimental spectrum reproduced in Fig. 1b of ref. [12]. The linewidth given by Coxon and Ramsay was 2.2 cm^{-1}, and it is encouraging, therefore, that the linewidths obtained photographically can be taken as reliable estimates of the true $\delta\nu$ values.

The absolute absorption cross-sections reported in the present work are based on measurements of the apparent extinction coefficient (ϵ) for absorption near the head of the 11–0 $^2\Pi_{3/2}$–$^2\Pi_{3/2}$ sub-band near 277 nm. Results from the two most recent studies by flash photolysis [5] and discharge-flow [6] methods agree to within 10%, and are considerably larger than the values obtained in earlier studies by flash photolysis [2 - 4]. A similar agreement was also obtained for absorption in the continuum at 256 nm. In the flow work, Clyne and Coxon [6] determined ClO concentrations by titration with NO or O atoms, and intensities were measured photoelectrically. These data are thus considered preferable to those obtained by the more difficult technique of plate photometry used in the flash photolysis experiments.

Clyne and Coxon's results for the 11–0 band were obtained with a spectral slit width of 43 cm^{-1}. The apparent extinction coefficient, defined according to eqn. (8):

$$\log_{10}(I_i/I_t) = \epsilon\, c\, l \qquad (8)$$

where c is the concentration (mol/l) and l is the path length (cm), was found to be ϵ (277 nm) = 1900 ± 60 l mol^{-1} cm^{-1} at 298 K. The interpretation of this value in terms of the more useful wavelength-dependent cross-section has been facilitated by computer-simulated determinations of absorption intensities under the conditions employed by Clyne and Coxon [6]. The results are given in Table 5, and were obtained using integration steps of 0.05 cm^{-1},

TABLE 5

Computed absorption intensities for the 11–0 $^2\Pi_{3/2}$–$^2\Pi_{3/2}$ sub-band of ClO(A–X).

Run	ν_2 (cm^{-1})	ν_1 (cm^{-1})	T (K)	$\delta\nu$ (cm^{-1})	$N \times 10^{-15}$ (cm^{-2})	$\sigma_0^{11} \times 10^{16}$ (cm^2)	I_t/I_i	$-\ln(I_t/I_i)$
1	36069	36026	300	2.0	2.0	4.0	0.9817	0.0185
2	36069	36026	300	2.0	4.0	4.0	0.9632	0.0375
3	36069	36026	300	2.0	8.0	4.0	0.9276	0.0752
4	36069	36026	300	1.0	8.0	8.0	0.9277	
5	36073	36030	300	2.0	8.0	4.0	0.9314	
6	36072	36029	300	2.0	8.0	4.0	0.9307	
7	36071	36028	300	2.0	8.0	4.0	0.9285	
8	36070	36027	300	2.0	8.0	4.0	0.9274	
9	36068	36025	300	2.0	8.0	4.0	0.9274	
10	36067	36024	300	2.0	8.0	4.0	0.9271	
11	36063	36020	300	2.0	8.0	4.0	0.9291	
12	36067	36030	300	2.0	8.0	4.0	0.9260	
13	36067	36035	300	2.0	8.0	4.0	0.9253	
14	36067	36040	300	2.0	8.0	4.0	0.9230	
15	36067	36024	300	2.0	5.8	3.7365	0.9500	0.513
16	36067	36024	200	2.0	6.41	3.7365	0.9278	0.0749
17	36067	36024	450	2.0	5.186	3.7365	0.9674	0.0331
18	36108	35560	300	2.0	5.8	3.7365	0.9885	
19	36108	35560	200	2.0	5.8	3.7365	0.9885	

with a 36 cm^{-1} integration width centred on each absorption line. Decrease of the step width, or increase of the integration width made no significant changes in the absorption intensities. Runs 1 - 3, in which the number of absorbers per unit cross-section (N) is varied, demonstrate that Beer's law holds remarkably well, as found experimentally [6]. Run 4 confirms the expectation that a change of linewidth ($\delta\nu$) is accommodated by a simultaneous change in $\sigma_{v'}^{v''}$ with inverse proportionality. Runs 5 - 11 differ from run 3 in the values chosen for the nominal centre frequency (ν_0) of the absorption experiment, although all the runs use the same 43 cm^{-1} spectral width. In the real experiment [6], the spectrometer was scanned for maximum absorption, and in agreement with Table 5, the intensity of absorption was insensitive to the precise value of ν_0.

Another interesting aspect of the experimental results which is tested in Table 5 is the weak dependence of the intensity of absorption on spectral slit width. This is shown in runs 12 - 14, in which spectral widths of 37, 32 and 27 cm^{-1} are employed. While there is a small increase in intensity of absorption with decreasing slit width, this would have been difficult to detect experimentally.

A typical result in the determination of ϵ (277 nm) was 5% absorption ($I_t/I_i = 0.95$) for l = 20 cm. With ϵ (277 nm) = 1900 l mol^{-1} cm^{-1}, the corresponding value of N for the $^2\Pi_{3/2}$ component is 5.80×10^{15} cm^{-2}.

It should be noted that the $^2\Pi_{1/2}$–$^2\Pi_{3/2}$ spin-orbit separation [21] is ~318 cm^{-1}, and leads to significant thermal populations of the $^2\Pi_{1/2}$ component. The population ratio $N(^2\Pi_{1/2}):N(^2\Pi_{3/2})$ is 1:4.6 at 300 K and 1:10 at 200 K. Run 15 shows that a value of $\sigma_{v''}^{v'} = 3.7365 \times 10^{-16}$ cm^2 reproduces an absorption of 5% for a linewidth of 2 cm^{-1}. In runs 16 and 17, the temperature is varied, and as expected, and found experimentally [6], the absorbance decreases with increase in temperature. From the expression given by Clyne and Coxon [6], the experimental value of $\epsilon(300\ K)/\epsilon(450\ K)$ is 1.53, which can be compared with the result in Table 5 of 1.56. The agreement is extremely satisfactory, and lends confidence to the calculations extrapolated below 300 K, as necessary in stratospheric applications.

The final two runs (18 and 19) in Table 5 give computed absorptions at 300 K and 200 K for a spectral width sufficiently large that more than 99% of the absorption of the sub-band is included. The value of I_t/I_i is 0.9885 for both temperatures. This result is required in calculating photolysis rates, as discussed later.

Profiles of absorption cross-sections for other bands can be generated using the information in Table 2. Data for the 2–0, 3–0 and 4–0 $^2\Pi_{3/2}$–$^2\Pi_{3/2}$ sub-bands are of particular interest as these bands might be detectable for stratospheric ClO. Results for these three sub-bands are shown in Figs. 3 - 5 for 200 K and 300 K. $\sigma_0^{v'}$ are found from the relation,

$$\frac{\sigma_0^{v'}}{\sigma_0^{11}} = \frac{R_e^2(\bar{r}_{v',0})\, q_{v',0}(\delta\nu)_{v'=11}}{R_e^2(\bar{r}_{11,0})\, q_{11,0}(\delta\nu)_{v'}} \qquad (9)$$

The variation of R_e^2 has been calculated recently by Arnold *et al.* [14]. Using the Franck–Condon factors in Table 2, the values of $10^{16}\ \sigma_0^{v'}$ are 1.025, 0.318 and 0.192 cm^2 for the 4–0, 3–0 and 2–0 bands with $\delta\nu$ = 1.5, 2.5 and 1.7 cm^{-1} respectively. The profiles for the 2–0 sub-band are similar in appearance to that for the 11–0 sub-band in Fig. 2; however, the cross-sections are lower, principally because of poorer Franck–Condon overlap. The profiles for the 3–0 and 4–0 sub-bands appear simpler because the P and R branches overlap in both cases. The narrower linewidth for the 4–0 band shows that structure in any absorption experiment at long wavelengths would probably be easier to identify than for the 2–0 and 3–0 bands.

Discussion

The absorption cross-sections found in the present work should be of much value in interpretation of both laboratory and atmospheric intensity data. The main sources of error are the uncertainty in Clyne and Coxon's [6] measurement of ϵ (277 nm) and in the Franck–Condon factors. It is unlikely that the combined error is greater than 15%. However, some mention should also be made of isotope effects. The calculations were performed for ^{35}ClO, and the results are thus strictly accurate only for this isotope. However, because of the small isotope splittings and large linewidths, which cause

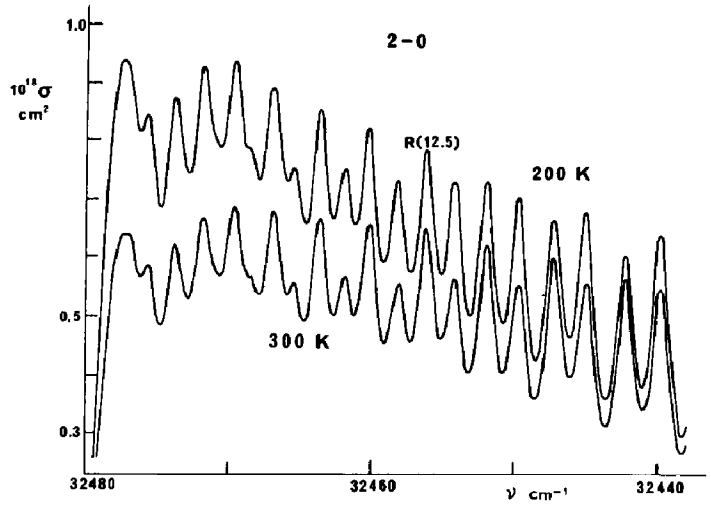

Fig. 3. Computed absorption cross-sections for the 2–0 ^{35}ClO ($A^2\Pi_{3/2}$–$X^2\Pi_{3/2}$) sub-band at 200 and 300 K. Linewidth = 1.7 cm^{-1}.

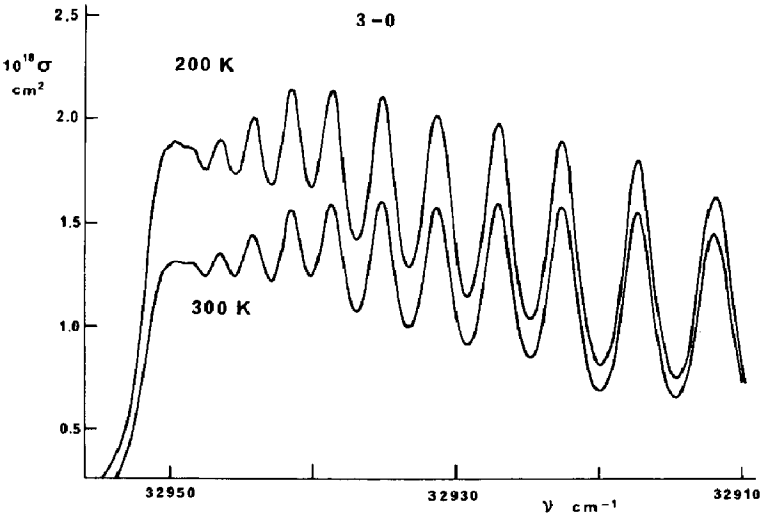

Fig. 4. Computed absorption cross-sections for the 3–0 ^{35}ClO ($A^2\Pi_{3/2}$–$X^2\Pi_{3/2}$) sub-band at 200 and 300 K. Linewidth = 2.5 cm^{-1}.

much blending of the rotational lines, only small error will arise in use of the cross-sections for natural chlorine.

It is of interest to calculate the bandhead absorption which might be observed for stratospheric ClO. On the basis of recent model calculations, the total column density of ClO ($^2\Pi_{3/2,v''} = 0$) is $\sim 10^{14}$ cm^{-2} [23]. Assuming a temperature of 220 K, intensities of absorption (I_t/I_i) of 0.99965 (0.035%), 0.99983 (0.017%) and 0.99992 (0.008%) are found for the 4–0, 3–0 and 2–0 bands respectively.

The extensive predissociation in ClO $A^2\Pi$ has been discussed by Coxon and Ramsay [12]. The large linewidths in the A–X system correspond to A

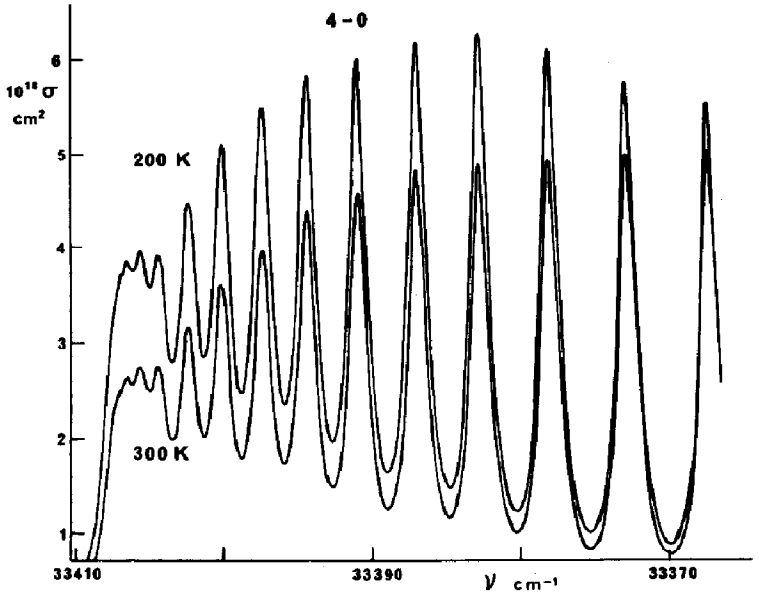

Fig. 5. Computed absorption cross-sections for the 4–0 ^{35}ClO ($A^2\Pi_{3/2}$–$X^2\Pi_{3/2}$) sub-band at 200 and 300 K. Linewidth = 1.5 cm^{-1}.

state lifetimes of a few ps, so that predissociation is several orders of magnitude more rapid than A → X fluorescence. The quantum yield for ClO photolysis is thus unity for band absorption as well as for the continuum. It is possible, therefore, to derive a simple procedure for the calculation of photolysis rates. The intensity distribution of the radiation is represented by $J(\nu)$, which is the photon flux per cm^2 per unit cm^{-1} interval. Runs 18 and 19 of Table 5 show that when $J(\nu)$ is independent of frequency, $I_t/I_i = 0.9885$ for $N(X^2\Pi_{3/2}) = 5.80 \times 10^{15}$ cm^{-2}. This result refers to the entire 11–0 $^2\Pi_{3/2}$–$^2\Pi_{3/2}$ sub-band over a 452 cm^{-1} spectral width. Since

$$I_{abs} = I_i - I_t \tag{10}$$

then

$$I_{abs} = I_i\,(1 - 0.9885)$$
$$= 452\,J\,(0.0115) \tag{11}$$

The absorption intensity can also be written as $I_t/I_i = e^{-\alpha N}$. α is found to be 2.0×10^{-18} cm^{-2}. Substituting in eqn. (10):

$$I_{abs} = 452\,I_i\,(1 - e^{-\alpha N}) \tag{12}$$

which simplifies accurately under optically thin conditions to:

$$I_{abs} = 9.04 \times 10^{-16}\,JN \tag{13}$$

In cases where J varies with frequency, as for example when considering the solar flux, an absorption would be more properly calculated by convolution of the flux with the absorption cross-section, and integration over all frequencies. In practice, however, it will usually be sufficiently accurate to use

$J(\nu)$ at the band origin in eqn. (13). In this case, the total absorption can be calculated by summing the contributions from all bands:

$$I_{abs}(\text{total}) = \frac{9.04 \times 10^{-16} N_{v''}}{R_e^2(\bar{r}_{11,0})\, q_{11,0}} \sum_{v',v''} J(\nu_{v',v''}) q_{v',v''} R_e^2(\bar{r}_{v',v''}) \qquad (14)$$

In applying eqn. (14), it is emphasized that $N_{v''}$ refer to the $^2\Pi_{3/2}$ component, and the expression thus gives the photolysis rate for ClO $^2\Pi_{3/2}$. However, since the origins for the $^2\Pi_{1/2}$ sub-bands are shifted by only ~ 200 cm^{-1} from those of $^2\Pi_{3/2}$, and since the $^2\Pi_{1/2}$ sub-bands make relatively small contributions, little error is introduced if $N_{v''}$ for total ClO $X^2\Pi$ is used to obtain total photolysis rates.

Acknowledgements

Grateful acknowledgement is made to the Trustees of the Killam Memorial Fund for support and a Research Professorship at Dalhousie University. Thanks are also due to the National Research Council of Canada for an operating grant.

References

1 G. Pannetier and A. G. Gaydon, Nature, 161 (1948) 242.
2 G. Porter and F. J. Wright, Discuss. Faraday Soc., 14 (1953) 23.
3 F. J. Lipscomb, R. G. W. Norrish and B. A. Thrush, Proc. R. Soc. (A), 233 (1956) 455.
4 F. H. C. Edgecombe, R. G. W. Norrish and B. A. Thrush, Proc. R. Soc. (A), 243 (1957) 24.
5 N. Basco and S. K. Dogra, Proc. R. Soc. (A), 323 (1971) 29, 401, 417.
6 M. A. A. Clyne and J. A. Coxon, Proc. R. Soc. (A), 303 (1968) 207.
7 M. A. A. Clyne and I. F. White, Trans. Faraday Soc., 67 (1971) 2068.
8 M. J. Molina and F. S. Rowland, Nature, 249 (1974) 810.
9 F. S. Rowland and M. J. Molina, Rev. Geophys. Space Phys., 13 (1975) 1.
10 R. W. Nicholls, J. Atmos. Sci., 32 (1975) 856.
11 J. A. Coxon, J. Photochem., 5 (1976) 337.
12 J. A. Coxon and D. A. Ramsay, Can. J. Phys., 54 (1976) 1034.
13 R. A. Durie and D. A. Ramsay, Can. J. Phys., 36 (1958) 35.
14 J. O. Arnold, E. E. Whiting and S. R. Langhoff, J. Chem. Phys., in press.
15 J. A. Coxon, W. E. Jones and E. G. Skolnik, Can. J. Phys., 54 (1976) 1043.
16 T. Amano, S. Saito, E. Hirota, E. Morino, Y. Johnson and F. X. Powell, J. Mol. Spectrosc., 30 (1969) 275.
17 J. A. Coxon, J. Quant. Spectrosc. Radiat. Transfer, 11 (1971) 443.
18 J. A. Coxon, J. Mol. Spectrosc., 50 (1974) 142.
19 J. A. Coxon, J. Quant. Spectrosc. Radiat. Transfer, 11 (1971) 1355.
20 R. N. Zare and J. K. Cashion, University of California Radiation Laboratory Report, UCRL-10881 (1963).
21 I. Kovács, Rotational Structure in the Spectra of Diatomic Molecules, Adam Hilger, London (1969).
22 N. Basco and R. D. Morse, J. Mol. Spectrosc., 45 (1973) 35.
23 R. T. Watson, personal communication (1976).